Inventory for Supplemental Information

Supplemental Data.

Supplemental Figure S1 – This figure is related to Figure 1 of the paper. This figure provides information regarding the gene *Rabex-5* described throughout the paper and reagents used in the paper to characterize the gene including loss-of-function mutant alleles referred to in the main text and used in Figures 1 and 2 as well as transgenic alleles we generated which are used in Figures 3 and 4. The phenotypes in Figure 1 were due primarily to *Rabex-5* RNAi mostly in females; in this figure we present additional data regarding males in the same experiments as well as the phenotypes caused by genomic deletion of the gene. We also present the corresponding quantification, quantification of additional experiments, and additional images.

Supplemental Figure S2 – This Table is related to Figure 2 of the paper. Figure 2 presented images of phenotypic enhancement of activated *Egfr* and activated Ras expression in differentiating cells in the eye upon loss of *Rabex-5*. This figure provides additional controls showing that the phenotypes of black tissue and lethality correspond to enhancement of the Ras expression phenotypes, and we show additional controls, quantification, and experiments.

Supplemental Figure S3 – This Table is related to Figure 3 of the paper. In this figure, we show immunohistochemical staining and Western analysis showing expression of the wild-type and mutant *Rabex-5* transgenes in the fly wing. In addition, we show increasing severity of the phenotype caused by *Rabex-5* expression upon increased temperature at which the transgenic flies were raised.

Supplemental Figure S4 – This figure is related to Figure 4 of the paper. In this figure, we show immunohistochemical staining and Western analysis showing expression of the wild-type and mutant *Rabex-5* transgenes in differentiating cells in the fly eye, as well as the morphology of adult eyes expressing these transgenes. We also present quantification of the effects of *Rabex-5* over-expression on flies expressing activated Ras and Raf in differentiating cells in the eye. In contrast to its suppression of activated Ras, *Rabex-5* does not suppress activated *Raf*. We also show additional controls showing the ability (or lack) of *Rabex-5* mutants to promote Ras ubiquitination, the inability of *Rabex-5* to promote ubiquitination of Rab5, and the lack of an unrelated ligase, DIAP1, to promote Ras ubiquitination.

Supplemental Experimental Procedures – Although the main text contains an Experimental Procedures section describing the techniques employed in the manuscript, this additional information provides more detailed explanations as to describing the techniques and how the experiments were conducted.

Supplemental References – This section of the Supplemental information contains 4 references cited in the Supplemental Experimental Procedures that were not cited in the main text.

Supplemental Data

Supplemental Figure S1A-B:

A

```
dm Rabex-5 1MSTAARPPSLRLGQQDLKCRSGCGFYGTPQNEGLCSMCFREKFNDKQRKLKQtggetgpg  60
           MS  +    + + Q DL C+ GCG+YG P  +G CS C+RE+++  ++K  Q   E
Hs Rabex-5 1MSLKSERRGIHVDQSDLLCKKGCGYYGNPAWQGFCSKCWREEYHKARQKQIQEDWE----  56

dm Rabex-5  ssssVATLDRRSPQHAHLQGKVEQQVRKPSDKEQDNLGTLQKKKFTAVLQKTLQAGAQ-- 118
               +A   +R  + A    +  Q  +  +  + +   T +K +    ++K   A ++
Hs Rabex-5  ----LAERLQREEEEAFASSQSSQGAQSLTFSKFEEKKTNEKTRKVTTVKKFFSASSRVG 112

dm Rabex-5  -KITQQRGHVPDPTEGQFLLQLRQLRIPDDGKRKLKLEI--------QRLDSDIRKYMNG  16
             K   Q    P P+        RQ  I  D   K  +E         Q +    + ++ G
Hs Rabex-5  SKKEIQEAKAPSPSIN------RQTSIETDRVSKEFIEFLKTFHKTGQEIYKQTKLFLEG  166

dm Rabex-5  NGGK---NINELSDLVQNAYTKVSDIVHNDPSFEIATNEDRDSAIDFFEKVVMTQNHKFL  226
              K   +I E S+  Q+ Y  V++ +           E  +  +D  EK +MT+ +K++
Hs Rabex-5  MHYKRDLSIEEQSECAQDFYHNVAERMQTRGK---VPPERVEKIMDQIEKYIMTRLYKYV  223

dm Rabex-5  FSPYFTTDEDSDVKVQKRIRQLSWITAKHLDCSIDEVNSEARDLVYNAISELVGIDSYYS  286
            F P  T DE  D+ +QKRIR L W+T + L   ++E   E  D+V  AI++++ +DS
Hs Rabex-5  FCPETTDDEKKDLAIQKRIRALRWVTPQMLCVPVNEDIPEVSDMVVKAITDIIEMDSKRV  283

dm Rabex-5  PQEKLQCTWRCCRHIFELLKRATGGPASADDFLPALIFVVLKANPVRLHSNINFVTRFTN  346
            P++KL C  +C +HIF  +K     PASADDFLP LI++VLK NP RL SNI ++TRF N
Hs Rabex-5  PRDKLACITKCSKHIFNAIKITKNEPASADDFLPTLIYIVLKGNPPRLQSNIQYITRFCN  343

dm Rabex-5  ASRLMSGESGYYFTNLCSAIAFIENLNGESLGVSSEEFEALMSGQ-QPYSTPWES-ALLA  404
             SRLM+GE GYYFTNLC A+AFIE L+ +SL +S E+F+  MSGQ  P     ES +  A
Hs Rabex-5  PSRLMTGEDGYYFTNLCCAVAFIEKLDAQSLNLSQEDFDRYMSGQTSPRKQEAESWSPDA  403

dm Rabex-5  CESLHLISENMKRMEMLQKRNALISSGITSFEKELIDFQREVTERVDTVIAKAPLNLLPI  464
            C  +  + +N+  +  L +R   I +     EK+LID+   +   V  ++ K PL + P
Hs Rabex-5  CLGVKQMYKNLDLLSQLNERQERIMNEAKKLEKDLIDWTDGIAREVQDIVEKYPLEIKPP  463

dm Rabex-5  KTP  467
              P
Hs Rabex-5  NQP  466
```

B

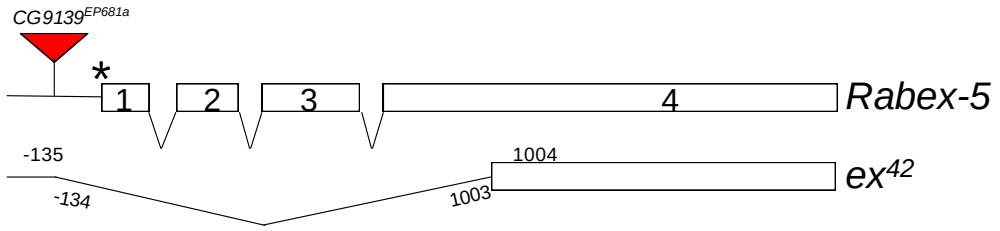

Supplemental Figure S1C-Z:

C

Genotype	Body Weight (males)	Wing Area (males)
Actgal4/+	1.000 ± 0.055 (163)	1.000 ± 0.062 (10)
Act>Rabex-5^{IR}	1.101 ± 0.019 (133)*	1.156 ± 0.067 (11)*
Act>Rabex-5^{IR}; Ras^{e1b}/+	1.030 ± 0.032 (47)†	1.109 ± 0.044 (13)†

D

Genotype	Extra PCV		Extra LV	
	Males	Females	Males	Females
Actgal4/+	0.0% (0/151)	1.6% (2/123)	0.0% (0/151)	0.0% (0/123)
Act>Rabex-5^{IR}	72% (18/25)*	94.7% (36/38)*	20% (5/25)*	18.4% (7/38)*
Act>Rabex-5^{IR}; Ras^{e1b}/+	0.0% (0/24)†	3.2% (1/31)†	0.0% (0/24)†	0.0% (0/31)†
Act>Rabex-5^{IR}; Ras^{e2f}/+	4.5% (1/22)†	8.3% (3/36)†	0.0% (0/22)†	0.0% (0/36)†
C765gal4/+ (30°C)	0.0% (0/132)	0.0% (0/102)	0.0% (0/132)	0.0% (0/102)
C765>Rabex-5^{IR} (30°C)	80.8% (105/130)*	80.6% (116/144)*	35.4% (46/130)*	73.6% (106/144)*
C765>Rabex-5^{IR}; Ras^{e1b}/+ (30°C)	1.4% (1/70)†	1.7% (1/58)†	0.0% (0/70)†	0.0% (0/58)†
C765gal4/+ (25°C)	0% (0/50)	0% (0/60)		
C765>Rabex-5^{IR} (25°C)	47.4% (36/76)*	70% (49/70)*		
C765>Rabex-5^{IR}; Ras^{e1b}/+ (25°C)	0% (0/34)†	0% (0/76)†		
Actgal4/+	0.0% (0/132)	0.0% (0/86)		
Act>Rabex-5^{IR}	21.1% (8/38)*	15.2% (7/46)*		
Act>Rabex-5^{IR}; Egfr^{k05115}/+	0.0% (0/16)†	6.3% (2/32)		
Act>Rabex-5^{IR}; sos^{e4g}/+	0.0% (0/20)†	ND		
Act>Rabex-5^{IR}; Ras^{e1b}/+	0.0% (0/24)†	0.0% (0/26)†		
Act>Rabex-5^{IR}; phl^{C110}/+	*ND*	0.0% (0/72)†		
Act>Rabex-5^{IR}; Dsor1^{S-122}/+	*ND*	0.0% (0/42)†		
Act>Rabex-5^{IR}; rl^{EMS698}/+	2.9% (1/34)†	3.1% (1/31)		

G

Genotype	Males with Extra PCV	Females with Extra PCV
y w hsFLP;FRT80BpW+UbiGFP/FRT80B	0.0% (0/164)	2.1% (4/194)
y w hsFLP;FRT80BpW+UbiGFP/FRT80B Rabex-5^{ex42}	24.8% (26/105)*	46.8% (59/129)*
y w hsFLP;rl^{EMS698}/+; FRT80BpW UbiGFP/FRT80B Rabex-5^{ex42}	8.3% (6/72)†	8.6% (9/105)†

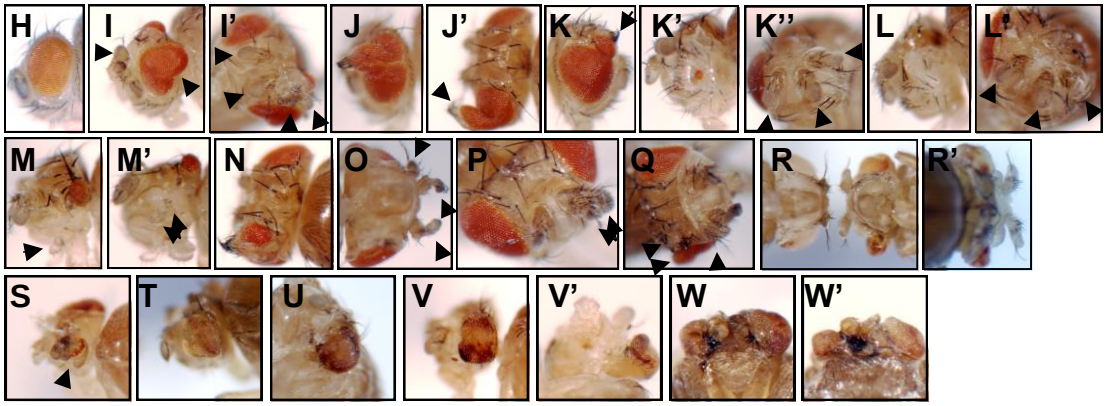

X

Genotype	% of eclosing flies of the genotype
y w eyFLP; FRT80B Mi55 UbiGFP/FRT80B Rabex-5^{ex42}	1.8% (2/110)*
y w eyFLP; rl^{EMS698}/+; FRT80B Mi55 UbiGFP/FRT80B Rabex-5^{ex42}	12.5% (4/32)†

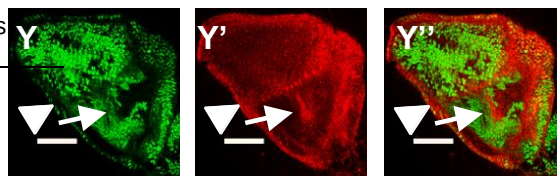

Z

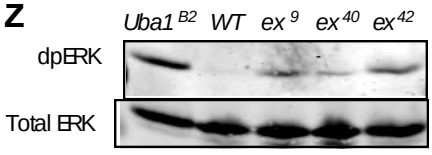

Z'

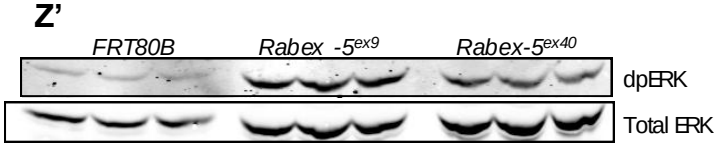

Supplemental Figure S1 (related to Figure 1): Reduction of *Rabex-5* by mutation and RNAi results in increased ERK activation and Ras/ERK-dependent phenotypes. A) BLAST search revealed *CG9139* as the closest *Drosophila* homolog of *homo sapiens Rabex-5.* BLAST alignment of *CG9139,* referred to here as *Rabex-5 (dm Rabex-5*, upper sequence) with human *Rabex-5 (hs Rabex-5*, lower sequence) is shown. Conserved residues F25, Y26 in *Drosophila* (Y25 Y26 in human, boxed in blue) were mutated to alanine in transgenic construct *Rabex-5^{FY}* used in Figs. 3-4 (see reference 9 of the main text). Conserved residues D316, P320, Y357, and T360 in *Drosophila* (D313, P317, Y354, and T357 in human, boxed in red) were mutated to alanine in transgenic construct *Rabex-5^{DPYT}* used in Figs. 3-4 (Delprato et al., 2004). B). Deletion allele *Rabex-5^{ex42}* was generated by imprecise excision as described in the Supplemental Experimental Procedures and lacks promoter regions, the start ATG, and much of the coding region. Genomic sequence is present 135 bases prior to the start ATG (base 1295891 of the genomic sequence) and resumes at 1004 bases into the corresponding mRNA (1297241 of the genomic sequence). C) Summary of *Act>Rabex-5^{IR}* phenotypes in male flies for experiment from Fig. 1D. As in Fig. 1D, body weight and wing area were normalized to 1.000 for controls and shown as a ratio to controls ± standard deviation; number of samples in parentheses. D) Summary table of wing phenotypes for indicated genotypes as described in Fig.1 including data for male wings. Also summarized are *c765gal4* experiments performed at 25ºC. *c765>Rabex-5^{IR}* PCV phenotype from male and female flies reared at 25°C is less severe than at 30°C (Fig. 1I, 1K) likely due to decreased expression of the inverted repeat transgene by the gal4/UAS system at the lower temperature. Mutation in Ras, *Ras^{e1b}*, dominantly suppressed the extra PCV phenotype of *c765>Rabex-5^{IR}* at both temperatures. Quantification of *Act>Rabex-5^{IR}* experiments adjusting the gene dosage for other components of Ras signaling is also listed, as

described in the main text. As shown in Fig. 1, constitutive RNAi of *Rabex-5* (*Act>Rabex-5^{IR}*) causes extra posterior crossveins. We created a stock containing both *Actgal4* and *Rabex-5^{IR}* elements that we crossed simultaneously to stocks carrying mutant alleles of various components of Ras signaling. Carrying both elements in the same stock resulted in a less strong wing vein phenotype than by keeping each element separately, but the trend remained the same. Mutations in components upstream of Ras, including *Egfr* and *sos,* as well as mutations in downstream components such as *polehole*/Raf, *Dsor1*/MEK, and *rolled*/ERK all dominantly suppressed the extra PCV phenotype. *Egfr^{k05115}*, *Ras^{e1b}*, *phl^{C110}*, *Dsor1^{S-122}* were from the Bloomington Stock Center. E-G) We created homozygous *Rabex-5^{ex42}* clones or control homozygous *FRT80B* clones randomly throughout the fly using a heat-shock inducible FLP (details in the Supplemental Experimental Procedures). (F) Homozygous *Rabex-5^{ex42}* wing clones (in flies of the genotype *y w hsFLP; FRT80B pW+ Ubi-GFP/FRT80B Rabex-5^{ex42}*) contained extra PCV but control *FRT80B* clones (in flies of the genotype *y w hsFLP; FRT80B pW+ UbiGFP/FRT80B*) (E) did not. G) Table quantifying phenotypes in E-F. Extra PCV were dependent on Ras signaling; mutation in *rolled*/ERK, *rl^{EMS698}*, dominantly suppressed the extra PCV phenotype. H) Control *ey>dcr2* eye, also shown in Fig. 1L. I-Q) Strongly reducing *Rabex-5* in the eye by RNAi using *eygal4* and *dcr2* (*ey>dcr2, Rabex-5^{IR}*) produces a range of phenotypes. I-J) Some eyes are overgrown (I) or exhibit outgrowths (J) or ectopic eyes (K) with duplications in nearby antennae (I', J'', K'). K-M) Other flies saw reduction in eye size (K', M, M') or even loss of the entire eye (L). I' shows an overhead view of the eye in I; J' shows an overhead view of eye in J; K'' shows an overhead view of the eyes in K, K'; L' shows an overhead view of the eye in L. M) In some flies, we saw duplication of other structures such as the maxillary palps (M, view from another angle, M'). N) At times eye tissue was observed outside of the normal eye area and may

represent duplication of the eye/an ectopic eye or that the eye has been divided/interrupted by other tissue (another example shown in K). O-P) Antennae were often increased in size or appeared to have reinitiated antennal growth after partially forming an antenna (two examples shown; O, from an angle underneath, P from an enlarged, overhead view). Q) An additional example from an overhead view of a bulging eye outgrowth and antennal abnormalities. Examples shown in Fig. S2H, S2K', and S2K'' also appear in main Fig. 1. R-W') We created eyes composed almost entirely of *Rabex-5^{ex42}* using the FLP/FRT system as described in the Supplemental Experimental Procedures. Very few *y w eyFLP; FRT80B Rabex-5^{ex42}/FRT80B Mi55* flies survived to adulthood; most died as giant larvae or giant pupae, similar to *Act>dcr2, Rabex-5^{IR}* and *Rabex-5^{ex42}/Rabex-5^{ex42}* flies. In flies that survived, mutant eyes composed primarily of homozygous *Rabex-5^{ex42}* tissue (in flies of the genotype *y w eyFLP; FRT80B Mi55 UbiGFP/FRT80B Rabex-5^{ex42},* right in R, enlarged dorsal view in R') were bulging and sometimes larger (upper eye in R) or smaller (lower eye in R). The antennae in these flies were abnormal and at times appeared much larger in size. These changes were not seen in eyes composed primarily of homozygous *FRT80B* tissue (flies of the genotype *y w eyFLP; FRT80B Mi55 UbiGFP/FRT80B* left in R). R') An enlarged dorsal view of the *y w eyFLP; FRT80B Rabex-5^{ex42}/FRT80B Mi55* fly shown in R highlighting the abnormal head pattern and focusing on the antennae. S-V') Additional examples of *y w eyFLP; FRT80B Mi55 UbiGFP/FRT80B* flies which survived to adulthood. As with *ey>dcr, Rabex-5^{IR}* flies, these eyes often showed abnormally shaped bulging eyes (S, T, U, V) sometimes with ectopic antenna (S, arrowhead) or outgrowths (U). V') Alternate view of the eye shown in V highlighting the abnormal shape of the eye. W-W') Pharate *y w eyFLP; FRT80B Mi55 UbiGFP/FRT80B* adults that failed to eclose were dissected from their pupal cases; they showed similar and stronger abnormalities as those

that survived. W) Ventral view of overgrown, bulging eyes and antennal abnormalities of *y w eyFLP; FRT80B Mi55 UbiGFP/FRT80B* pharate adult, and (W') dorsal view of the same fly. In many cases, the tissue was so overgrown and abnormal that eye and antennal structures could not be identified in these adults (not shown). For R-W', white tissue represents homozygous *FRT80B* (R, left) or homozygous *FRT80B Rabex-5^{ex42}* tissue (R right, R'-W'), while red tissue represents either homozygous *FRT80B Mi55 UbiGFP* tissue or heterozygous tissue that did not undergo mitotic recombination. X) Table of mosaic flies surviving from R-V' from one representative experiment from several independent trials. Mendelien genetics predicts that 33% of the flies from a cross of *w; FRT80B Rabex-5^{ex42}/TM6B* x *y w eyFLP; FRT80B pW+ Mi55/TM6B* should be of the genotype *y w eyFLP; FRT80B Rabex-5^{ex42}/FRT80B pW+ Mi55.* However, reproducibly, this cross yielded no or very few flies of this genotype (typically under 2% of all flies to eclose). Mutation in *rolled/*ERK dominantly suppressed this lethality. For tables in C, D, G, and X, * indicates statistically significant difference compared to control ($p<0.05$); † indicates statistically significant suppression by the mutations indicated ($p<0.05$). Y-Y'') *y w eyFLP; FRT80B Rabex-5^{ex42}/FRT80B pW+ Ubi GFP* mosaic larval eye discs were stained for dpERK (red in Y', Y''). GFP (green in Y, Y'') indicates homozygous wild-type control *FRT80B pW+ Ubi GFP* tissue, while GFP negative (dark in Y, Y'') indicates homozygous *FRT80B Rabex-5^{ex42}* mutant tissue. Mosaic discs with small mutant clones appeared normal and showed no dpERK abnormalities (not shown) whereas mosaic discs with large mutant clones were often overgrown and folded (Y-Y'') making staining difficult to interpret. As shown in this example, many larger *FRT80B Rabex-5^{ex42}* mutant clones often contained strong dpERK staining (arrow) anterior to the furrow. Although the dpERK changes occurred in folded discs, as shown, the dpERK increase typically occurred along or within clonal boundaries. Y'') Merge of Y and Y'.

Scale bar indicates 50 μm. Z-Z') Staining with dpERK antibodies (upper panels) showed increased ERK activation in mutant larvae as shown in Fig. 1Q. Each blot was stripped and reprobed for total ERK (lower panels). Z) Representative Western blot of larvae homozygous for positive control *Uba1*^{B2} [21], negative control *FRT80B*, and mutant alleles *Rabex-5*^{ex9}, *Rabex-5*^{ex40}, and *Rabex-5*^{ex42} (left panels) showing each mutant side by side with controls. *Uba1*^{B2} is a hypomorphic allele of *Uba1*, the Ubiquitin Activating Enzyme. We showed previously that homozygous *Uba1*^{B2} mutant larvae show dramatic increased ERK activation (see reference 21 of the main text). *Uba1*^{B2} mutant larva is included here as a positive control. Z') Larvae for each mutant allele were examined in triplicate as shown for *Rabex-5*^{ex42} in Fig. 1Q, and here for *Rabex-5*^{ex9}, and *Rabex-5*^{ex40}. Images were analyzed using Image J software to quantify band intensities. Individual slices were taken from each band for both dpERK and total ERK. Total ERK levels from control *FRT80B* larvae were used to normalize the ERK levels. The ratio of adjusted dpERK for each mutant larva compared to the average dpERK from control larvae was calculated. Using this method, we calculated that *Rabex-5*^{ex9} mutant larvae showed 4.9 ± 0.44 (standard deviation)-fold increase compared to *FRT80B* larvae, and that *Rabex-5*^{ex40} mutant larvae showed an average 2.6 ± 0.18 (standard deviation)-fold increase compared to *FRT80B* control larvae.

Supplemental Figure 2A-J:

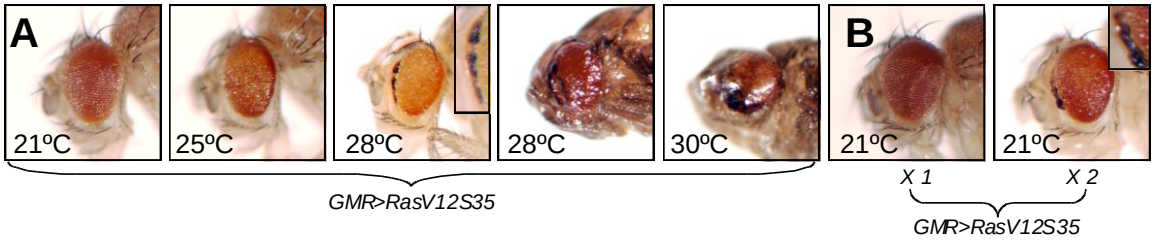

C

Genotype	Male eyes with black tissue **21°C**	Female eyes with black tissue **21°C**	Male eyes with black tissue **25°C**	Female eyes with black tissue **25°C**	Male eyes with black tissue **28°C**	Female eyes with black tissue **28°C**	Pharate eyes with black tissue **28°C**	Pharate eyes with black tissue **30°C**
w; GMRgal4, UAS RasV12S35 /SM6-TM6B	0.0% (0/52)	0.0% (0/44)	10.8% (16/148)	1.6% (3/186)	NA	100% (8/8)	100% (96/96)	100 % (62/62)
w; GMRgal4, UAS RasV12S35/ GMRgal4, UAS RasV12S35	NA	100% (6/6)	NA	NA	NA	NA	100% (44/44)	100% (6/6)

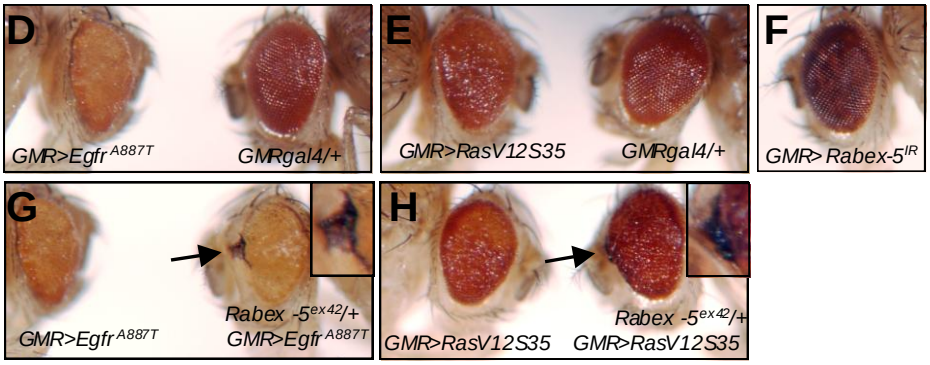

I

Genotype	Male eyes with black tissue	Female eyes with black tissue
GMRgal4/+	0%(0/200)	0% (0/200)
GMR>Rabex-5^{IR}	0% (0/100)	0% (0/100)
GMR>Egfr^{A887T}	0% (0/52)	0% (0/68)
GMR> Egfr^{A887T}; Rabex-5^{ex42}/+	45% (9/20)*	30% (6/20)*
GMR> Egfr^{A887T}, Rabex-5^{IR}	36% (8/22)*	13% (4/32)*
GMR>RasV12S35	1% (1/86)	0% (0/100)
GMR>RasV12S35; Rabex-5^{ex42}/+	3% (1/38)	0% (0/40)
GMR>RasV12S35, Rabex-5^{IR}	50% (1/2)*	37% (20/54)*
GMR>Raf^{gof}	45.2% (19/42)	40.4% (21/52)
GMR>Raf^{gof}; Rabex-5^{ex42}/+	41.2% (14/34)	35.3% (12/34)
GMR>Raf^{gof}, Rabex-5^{IR}	64.3% (9/14)	37.5% (12/32)

J

Genotype	% eclosing (observed)	Expected Mendelian frequency	% eclosing (normalized to control)
GMR>Egfr^{A887T}	50% (125)	50%	100% (125)
GMR>Egfr^{A887T}, Rabex-5^{IR}	29% (94)	50%	58% (94)*
GMR>RasV12S35	68% (139)	50%	100% (139)
GMR>RasV12S35, Rabex-5^{IR}	32% (84)	50%	47% (84)*

Supplemental Figure 2K-S:

K

Genotype	% eyes with strong phenotypes 18°C	Expected Mendelian frequency	% eclosing (normalized to control) at 18°C	% eclosing (normalized to control) 21°C
ey> RasV12S35	17% (52)	33%	100% (115)	100% (112)
ey>RasV12S35, Rabex-5^{IR}	38% (24)	33%	58% (86)	44% (123)

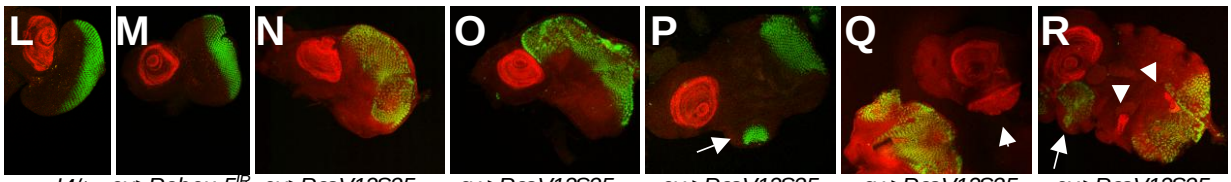

eygal4/+ *ey>Rabex-5^{IR}* *ey>RasV12S35* *ey >RasV12S35 + Rabex-5^{IR}* *ey >RasV12S35 +Rabex-5^{IR}* *ey >RasV12S35 +Rabex-5^{IR}* *ey >RasV12S35 +Rabex-5^{IR}*

S

Genotype	% of dissected larval eyes that show dramatic (more than 2X control) overgrowth	% of dissected larval eyes that show extra antenna	% of dissected larval eyes that show ectopic eyes
eygal4/+ (n=29)	0%	0%	0%
ey>Rabex-5^{IR}/+ (n=31)	0%	0%	0%
ey>RasV12S35 (n=34)	32%*	11%*	0%
ey>RasV12S35, Rabex-5^{ex42}/+ (n=44)	34%	14%	2%***
ey>RasV12S35, Rabex-5^{IR} (n=51)	49%***	16%	14%***

Supplemental Fig. S2 (related to Fig. 2): Loss of *Rabex-5* enhances activated *Egfr* and oncogenic Ras. A-C) Increasing severity of the *GMR>RasV12S35* phenotype results in increased roughening, the appearance of black tissue in the eyes, and an increase in lethality. We demonstrated the increased severity in two ways: first, by modulating temperature at which the flies were raised, and second, by increasing the dosage of the gal4/UAS elements. Three recombinant lines containing both *GMRgal4* and *UAS RasV12S35* elements on the second chromosome were balanced over the fused balancer *SM6-TM6B*. We raised these balanced stocks at 21ºC, 25ºC, 28ºC, and 30ºC and scored the presence/absence of black tissue in the eyes

and also scored number of pupal cases (for 28ºC and 30ºC) or adult flies (for 21ºC, 25ºC, and 28ºC) for *w; GMRgal4, UAS RasV12S35/SM6-TM6B* and *w; GMRgal, UAS RasV12S35/GMRgal, UAS RasV12S35* genotypes. A) The roughness and the number of eyes containing black tissue increased with temperature at which the flies were raised. B) The roughness and the appearance of black tissue in the eyes also increased with increased gene dosage of the *GMRgal4* and *UAS RasV12S35* elements. In all three recombinants, the trend of increased roughness, black tissue, and lethality was the same. C) Table summarizing the results from A-B for one of the three recombinants. The number of eyes with black tissue over the total number of eyes is shown in parentheses. Total number of eyes also reflects the number of flies examined (divided by 2) which indicates that the lethality increased with both increased temperature and increased dosage of the *GMRgal4* and *UAS RasV12S35* elements. Because increased temperature increases expression of the *RasV12S35* transgene, as does increased transgene dosage, the lethality and appearance of black tissue both likely reflect enhancement of the GMR>*RasV12S35* phenotype. NA = not available (due to lethality). D) Expressing activated *Egfr*, $Egfr^{A887T}$, in differentiating eye cells (*GMR*>$Egfr^{A887T}$) resulted in small, bulging, rough eyes with unstructured tissue (left, also shown in Fig. 2A left) compared to controls (*GMRgal4/+,* right). G) *Rabex-*5^{ex42} (right) enhanced *GMR*>$Egfr^{A887T}$, evident by the appearance of black tissue (arrows; enlarged in inset to the upper right). E) Expressing *RasV12S35* in differentiating eye cells (*GMR>RasV12S35*) resulted in smaller rough eyes (left, also shown in Fig. 2B left) compared to controls (*GMRgal4/+*, right). H) *Rabex-*5^{ex42} (right) enhanced *GMR>RasV12S35*, evident by the increased frequency of black tissue (arrows, enlarged in insets to upper right). F) *Rabex-5* RNAi in differentiating eye cells, *GMR>Rabex-*5^{IR}*,* showed no obvious phenotype. I) Table quantifying effects in both males and females of *Rabex-5* loss (by

mutation in one copy of *Rabex-5* or driving RNAi to *Rabex-5)* on $Egfr^{A887T}$, *RasV12S35,* and Raf^{gof}. *statistically significant difference compared to control ($p<0.05$). For Raf^{gof} experiments, *Rabex-5* reduction did not cause a statistically significant change in frequency of black tissue compared to control ($p>0.05$). Female eyes are shown in A-B, D-F, H; male eyes in G. J) Increasing the severity of activated *Egfr* expression or activated Ras expression in the eye causes increased lethality. Rearing these flies at 30°C often results in pupal lethality due to increased expression of the transgenes by the gal4/UAS system as shown for Ras in A-B. Reduction of *Rabex-5* by RNAi significantly enhanced the lethality of both activated *Egfr* (*GMR>*$Egfr^{A887T}$*)* and activated Ras (*GMR>RasV12S35)*. Crosses were designed to produce the same expected percentage of *GMR>*$Egfr^{A887T}$ or *GMR>RasV12S35* progeny from each cross (50% according to Mendelian ratios, middle column). Total progeny were counted from each cross, and the observed percentages of *GMR>*$Egfr^{A887T}$ or *GMR>RasV12S35* progeny were determined (left data column). Numbers were normalized to 100% for controls for comparison (right data column).* indicates statistically significant difference compared to control ($p<0.05$). K-R) Using *eygal4* to drive the *UAS RasV12S35* transgene to express oncogenic Ras in the early eye (*ey>RasV12S35)* can result in hyperplastic growth (see reference 16 of the main text), and other abnormalities including eye to antennal switch (see reference 17 of the main text) as reviewed in the main text. Increased expression of *RasV12S35* can also promote ectopic eye formation and cause pupal lethality. K) Table summarizing the effects of *Rabex-5* loss on *ey>RasV12S35* phenotypes in terms of adult eye phenotypes observed and lethality. RNAi of *Rabex-5* dramatically enhanced the strong eye phenotypes (dramatically overgrown eyes, antennal switches, ectopic eyes). In experiments designed to produce the same expected percentage of *ey>RasV12S35* progeny from each cross (33% according to Mendelian ratios), reduction of

Rabex-5 by RNAi significantly increased the lethality of *ey>RasV12S35* at the two temperatures tested (18°C and 21°C). L-R) Larval eye discs were dissected and stained with antibodies to *Distal-less* (to label presumptive antennal tissue, red) and antibodies to ELAV (to label presumptive photoreceptors, green). L-N) Control eye discs (also shown in Fig. 2D-F). L) *eygal4/+*. M) *ey>Rabex-5^{IR}*. N) Eye disc expressing *RasV12S35* in the early eye (*ey>RasV12S35*). O-R) Eye discs expressing *RasV12S35* undergoing RNAi to *Rabex-5* *(ey>RasV12S35, Rabex-5^{IR}*). (O,) Reduction of *Rabex-5* enhanced the dramatic overgrowth phenotype of *RasV12S35* expression, (P) promoted the formation of ectopic eyes, (Q) promoted the formation of ectopic antennae, and (R) sometimes resulted in multiple enhanced phenotypes in the same eye. S) Table summarizing the enhancement of *RasV12S35* early eye phenotypes by *Rabex-5* loss in dissected larval eye discs from L-R. Introducing the mutant allele *Rabex-5^{ex42}* statistically significantly dominantly enhanced the *ey>RasV12S35* phenotype in terms of the formation of ectopic eyes compared to control *RasV12S35* eye discs. RNAi to *Rabex-5* statistically significantly enhanced the *ey>RasV12S35* in terms of dramatic overgrowth, and formation of ectopic eyes compared to control *RasV12S35* eye discs. In the Table in S, * indicates statistically significant difference in phenotypes of *ey>RasV12S35* eye discs compared to control *eygal4/+* or control *ey>Rabex-5^{IR}* eyes discs. *** indicates statistically significant enhancement of *ey>RasV12S35* eye disc phenotypes by reduction in *Rabex-5.* Mouse monoclonal Anti-*Dll* antibodies (1:500) were generously provided by Jun Wu. Rat anti-ELAV antibodies (1:500) were from the DSHB.

Supplemental Figure S3:

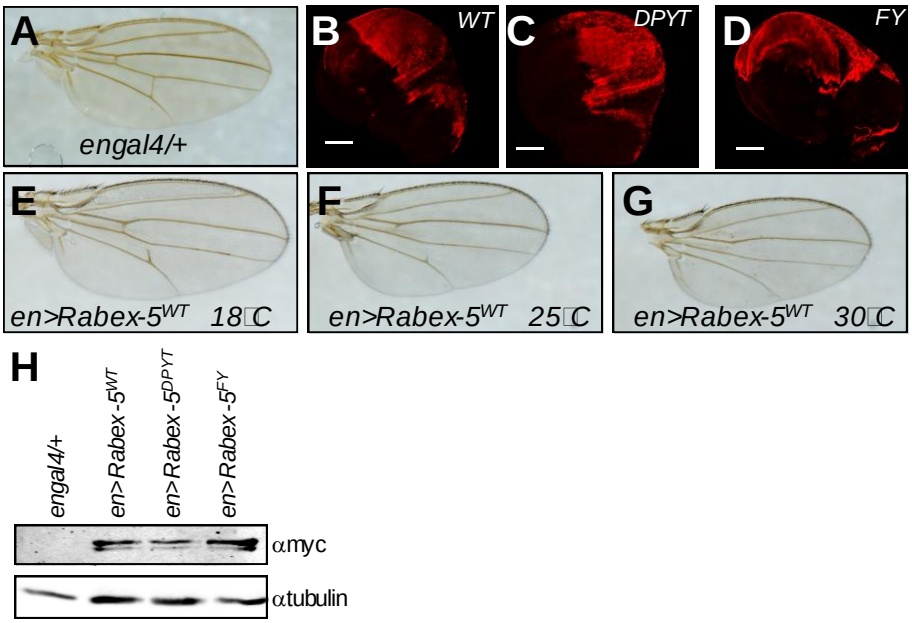

Supplemental Fig. S3 (related to Fig. 3): *Rabex-5* over-expression promotes loss of wing veins. A) Control *engal4/+* wing showing normal wing vein pattern. (B-D) Wing discs from third instar larvae stained with anti-myc antibodies (red) showed similar *engal4*-driven expression and primarily membrane localization of *Rabex-5*^{WT} (B) *Rabex-5*^{DPYT} (C), and *Rabex-5*^{FY} (D). Scale bars indicate 100 μm. Higher temperatures increase gal4/UAS-mediated expression. (E-G) As shown in Fig. 3B, *en>Rabex-5*^{WT} wings showed loss of wing veins. A stronger phenotype was seen at 30°C (G) than at 25°C (F) or 18°C (E). (H) Western blot showing *Rabex-5* transgene levels driven by *engal4* in larval wing discs

Supplemental Figure S4A-L:

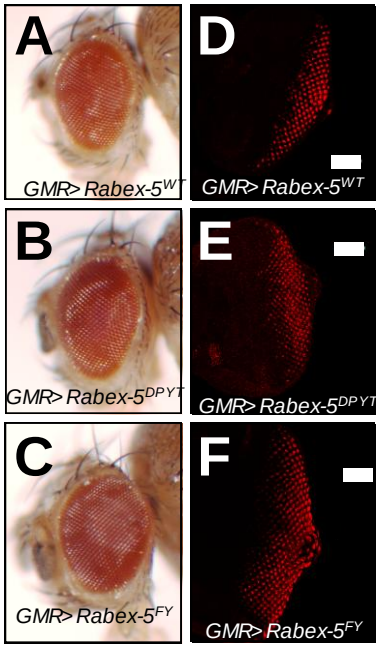

G

Genotype	Male eyes with substantial black patches	Female eyes with substantial black patches
GMRgal4/+	0.0% (0/86)	0.0% (0/102)
GMR>Rabex-5^{WT}	0.0% (0/62)	0.0% (0/90)
GMR>Rabex-5^{DPYT}	0.0% (0/44)	0.0% (0/44)
GMR>Rabex-5^{FY}	0.0% (0/22)	0.0% (0/34)
GMR>RasV12S35	61.1% (11/18)*	29.5% (23/78)*
GMR>RasV12S35, Rabex-5^{WT}	45.3% (39/86)†	19.3% (17/88)†
GMR>RasV12S35, Rabex-5^{DPYT}	26.7% (23/86)†	5.6% (6/108)†
GMR>RasV12S35, Rabex-5^{FY}	*ND*	70.8% (17/24)*
GMR>Raf^{gof}	28.1% (18/64)	26.6% (25/94)
GMR>Raf^{gof}, Rabex-5^{WT}	42.9% (18/42)	70.3% (52/74)

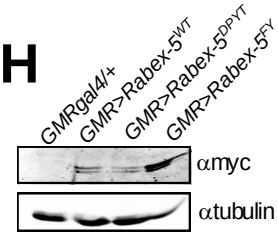

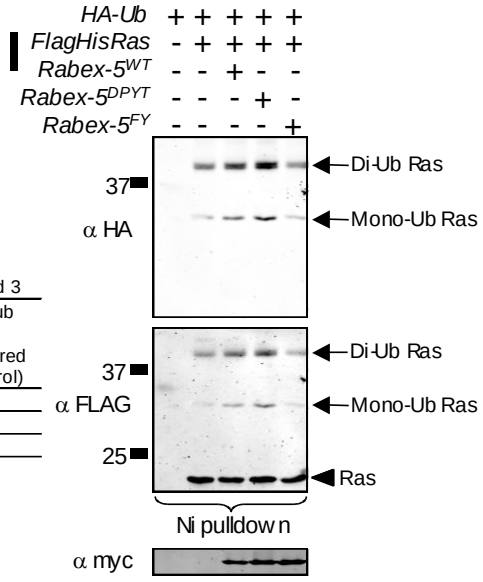

J

	Method 1	Method 2				Method 3
	% di-ub Ras (compared to control)	Un-conjugated Ras (%)	mono-ub Ras (%)	di-ub Ras (%)	% di-ub Ras (compared to control)	% di-ub Ras (compared to control)
Control	100	74.55	4.93	20.52	100	100
Rabex-5^{WT}	174	58.16	7.95	33.89	165	212
Rabex-5^{DPYT}	206	54.62	12.02	33.66	163	222
Rabex-5^{FY}	92	74.62	4.24	21.14	103	103

K

	% di-ubiquitinated Ras (compared to control)	% di-ubiquitinated Ras (compared to control)	% di-ubiquitinated Ras (compared to control)
Control	100 ± 0.0	100 ± 0.0	100± 0.0
Rabex-5^{WT}	256 ± 62*	210 ± 18*	265 ± 45*
Rabex-5^{DPYT}	231 ± 58*	188 ± 8.6*	238 ± 29*
Rabex-5^{FY}	107 ± 43	106 ± 30	111 ± 42

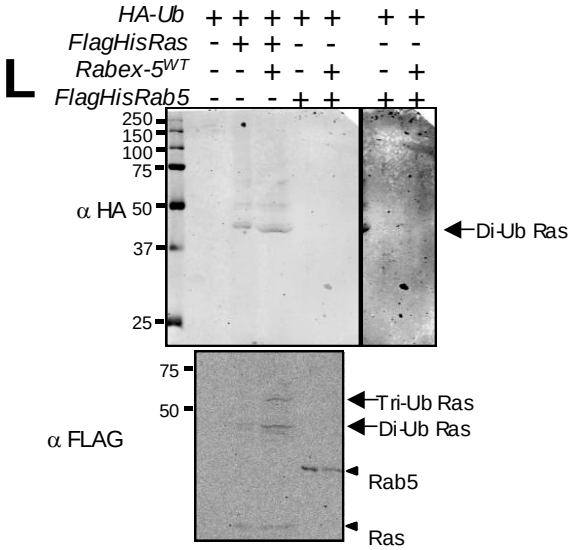

Supplemental Figure S4M-N:

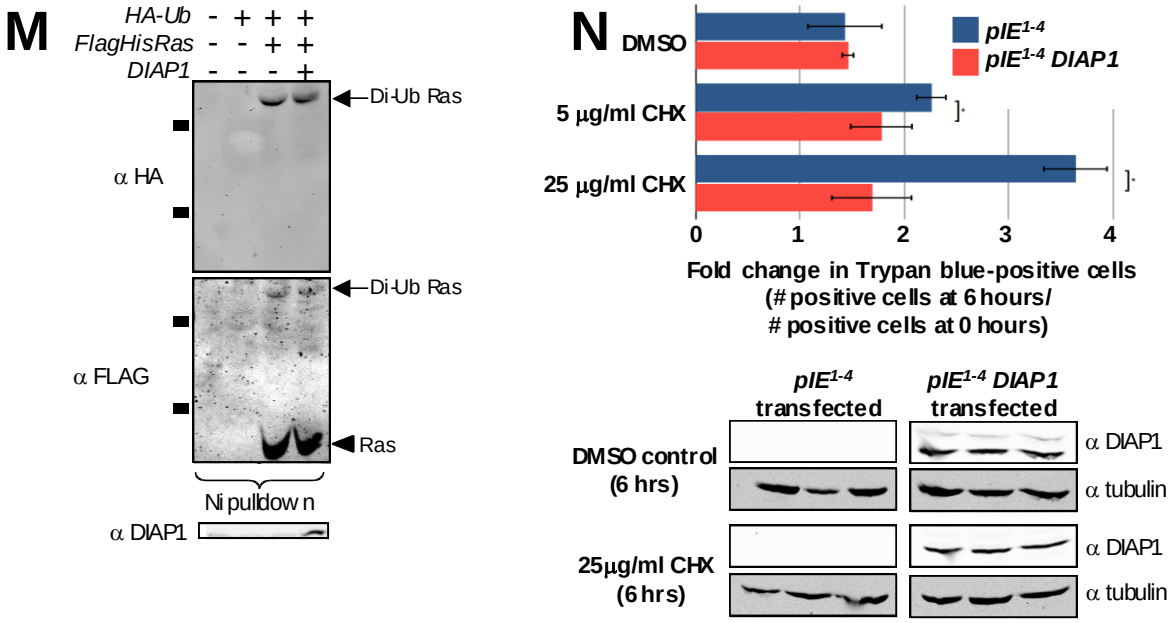

Supplemental Fig. S4 (related to Fig. 4): Rabex-5 promotes Ras ubiquitination via its ubiquitin ligase domain but does not promote Rab5 ubiquitination. A) *GMRgal4*-mediated expression of *Rabex-5^{WT}*, (B) *Rabex-5^{DPYT}*, or (C) *Rabex-5^{FY}* did not cause obvious phenotypes. Female eyes are shown. D-F) Eye discs from third instar larvae stained with anti-myc antibodies (red) showed similar *GMRgal4*-driven expression and localization of (D) *Rabex-5^{WT}*, (E) *Rabex-5^{DPYT}*, and (F) *Rabex-5^{FY}*. Scale bars indicate 50µm. G) Summary table including male eye phenotypes from experiments shown in Fig. 4A-D. *statistically significant difference for *Rabex-5* and/or *RasV12S35* transgene expression compared to *GMRgal4/+* control ($p<0.05$).† statistically significant suppression of *GMR>RasV12S35* ($p<0.05$). *ND* = not determined. H) Western blot of *Rabex-5* transgene levels driven by *GMRgal4* in third instar larval eye discs. Similar to the staining in D-F, western analysis indicates that the lack of suppression of *RasV12S35* by *Rabex-5^{FY}* in Fig. 4C-D and Fig. S4G does not result from lack of *Rabex-5^{FY}* protein expression. I) Nickel pulldown of lysates from cells expressing tagged Ras, Ub, and

Rabex-5 wild-type or mutant forms. As shown in Fig. 4E, wild-type *Rabex-5* expression increases Ras ubiquitination (right lane). Similarly, *Rabex-5*^{DPYT} also increases Ras ubiquitination, but *Rabex-5*^{FY} (the form with a mutant ubiquitin ligase domain) does not increase Ras ubiquitination. Anti-HA (upper panel), anti-FLAG (lower panel) staining; di-ubiquitinated Ras, arrows; unconjugated Ras, arrowhead. Anti-myc blot shows relative expression of the *Rabex-5* wild-type and mutant proteins indicating that the failure to promote Ras ubiquitination does not result from a lack of *Rabex-5*^{FY} protein expression. J-K) Quantifying the increase in Ras ubiquitination in cells is complicated; unlike ubiquitination assays in a purified system where the levels of each component can be carefully controlled, living cells may produce different levels of transfected plasmids, de-ubiquitinating enzymes may remove ubiquitin after it is conjugated, proteasome activity may result in normal protein turnover, etc. Therefore, we quantified the increase in Ras ubiquitination in three ways: first, we measured band intensities for unconjugated, mono- and di-ubiquitinated Ras and then calculated the ratio of di-ubiquitinated Ras to unconjugated Ras; second, we calculated the relative distribution of Ras between unconjugated, mono- and di-ubiquitinated forms; third, by using the level of unconjugated Ras to normalize the load for each lane, we adjusted the level of di-ubiquitinated Ras accordingly. (J) Quantification for these three methods is summarized for the data appearing in (I). K) Average increase in Ras di-ubiquitination using the three methods from a series of experiments is shown ± variance. * statistically significant increase compared to control. Importantly, all three methods showed a statistically significant increase in Ras di-ubiquitination in the presence of wild-type *Rabex-5* and *Rabex-5*^{DPYT} but no statistically significant difference ($p > 0.05$) between control and *Rabex-5*^{FY}. The lack of effect on Ras ubiquitination was not due to a failure to express *Rabex-5*^{FY}. *Rabex-5*^{FY} levels were similar or greater than *Rabex-5*^{WT} and *Rabex-5*^{DPYT}. L)To

address if *Rabex-5* promotes ubiquitination of close binding partners without specificity, we performed ubiquitination assays using Flag-6His-tagged Rab5. Flag-6His-tagged Rab5 was purified on nickel resin (as described for Flag-6His-tagged Ras). Shown are anti-HA western blot (upper panel) and anti-FLAG (tag on Rab5 and Ras, lower panel); arrowheads indicate unconjugated Ras and Rab5. Under conditions where *Rabex-5* promotes ubiquitination of Ras (arrows), no ubiquitination is seen for Rab5 (right panels). An over-exposure of the Rab5 panels from the anti-HA blot is shown to the right. No obvious ubiquitin conjugates are seen for Rab5 in the presence or absence of *Rabex-5* even in the over-exposure. The failure of *Rabex-5* to promote ubiquitination of Rab5 is consistent with data for mammalian *Rabex-5* (see reference 23 of the main text). M) To further address specificity, we over-expressed DIAP1, another ubiquitin ligase, in S2 cells and performed nickel pulldowns of lysates from cells expressing tagged Ras, ubiquitin, and DIAP1 as described in S4I and S4L. Unlike wild-type *Rabex-5*, DIAP1 expression does not increase Ras ubiquitination (right lane). Anti-HA (upper panel), anti-FLAG (lower panel) staining; di-ubiquitinated Ras, arrows; unconjugated Ras, arrowhead. Anti-DIAP1 blot (lowest panel) shows relative DIAP1 over-expression (right lane) compared to endogenous DIAP1 protein (left-most three lanes) to ~7.5 times endogenous levels. Despite the high over-expression of DIAP1, levels of Ras ubiquitination are not affected, indicating that not all ubiquitin ligases are capable of promoting Ras ubiquitination. It is well-accepted that DIAP1 expressed in this manner produces active protein (Wilson et al., 2002; Hays et al., 2002; Ditzel et al, 2008) capable of preventing cell death largely by targeting the caspase DRONC for ubiquitination and subsequent degradation. N) To confirm activity of DIAP1, we induced apoptosis using cycloheximide (CHX) in control-transfected and DIAP1-transfected cells and used Trypan Blue to determine the proportion of dying cells after 6 hours of treatment with

CHX. This experiment was performed in triplicate. In DIAP1-transfected cells (red), we see a reduction in the proportion of dying cells compared to control-transfected cells (blue) as indicated by incorporation of Trypan blue at 0 hours and 6 hours after treatment with 0 μg/ml (DMSO control), 5 μg/ml or 25 μg/ml CHX. DIAP1-transfected cells showed statistically significantly increased survival in the presence of CHX as shown in the bar graph. The values reflect the ratio of Trypan blue-positive cells at 6 hours to the number of Trypan blue-positive cells at 0 hours. There was no statistically significant difference between the proportion of Trypan blue-positive vector-transfected and DIAP-1 transfected cells treated with a DMSO control for 6 hours reflecting similar responses to the DMSO and transfection itself. Importantly, the DIAP1-transfected cells showed no statistically significant difference between the proportion of Trypan blue-positive cells upon control (DMSO) treatment and those undergoing treatment with 25 μg/ml CHX after 6 hours of treatment suggesting that the CHX did not promote a statistically significant increase in cell death in the presence of DIAP1. Below the bar graph are Western blots using anti-DIAP1 and anti-tubulin antibodies of lysates from cells transfected with vector control (left panels) or *DIAP1* (right panels) after 6 hours of treatment with a DMSO control or 25 μg/ml CHX showing high over-expression of DIAP1 protein in *DIAP1*-transfected cells. As indicated, these experiments were performed in triplicate. Rabbit anti-DIAP1 antibodies (used at 1:500) were generously provided by Hyung-Don Ryoo from NYU.

Supplemental Experimental Procedures:

***Drosophila* husbandry and *Drosophila* transgenic lines:** Flies were raised on standard media at 25°C except where otherwise indicated. The *UAS Raf*^{gof} transgene (acquired from the Bloomington Stock Center) encodes an N-terminally deleted form of *Drosophila Raf* (*polehole*). Deletion of the N-terminal negative regulatory region of *Raf* creates a constitutively active form of *Raf* kinase (see reference 20 of the main text), so the *UAS Raf*^{gof} transgene allows inducible expression of constitutively active *Raf.*

Generation of *Rabex-5* deletion alleles: To generate deletion alleles of *Rabex-5,* we obtained an insertion allele, *w*^{1118}*; P{EP}CG9139*^{EP681a}. *w*^{1118}*; P{EP}CG9139*^{EP681a} *P{EP}slmb*^{EP681b} from the Bloomington stock center. Hobo-mediated transposition can remove P-insertions from insertion sites (excision events). Some excision events remove the inserted sequences and also surrounding genomic DNA. We recombined the *P{EP}CG9139*^{EP681a} insertion (red inverted triangle) away from the *P{EP}slmb*^{EP681b} insertion in the original stock and onto the *FRT80B* chromosome. *w*^{1118}; *FRT80B P{EP}CG9139*^{EP681a} male flies were crossed to *y w; Hobo [pΔ2,3]; Dr/TM3* virgin female flies. *Hobo [pΔ2,3]/+; FRT80B P{EP}CG9139*^{EP681a}*/TM3* males were crossed to *w; pW+ /SM6-TM6B* virgin females. White-eyed *SM6-TM6B* progeny without TM3 markers were isolated and individually balanced. Three excision lines contained deletion of only *Rabex-5* (confirmed by diagnostic PCR). The *P{EP}CG9139*^{EP681a} insertion was 5' of the start ATG (asterisk); excision events removed promoter regions, the start ATG, and much of the coding region. The deletion in *Rabex-5*^{ex42}*,* used throughout the paper is shown schematically in Fig. S1B. In *Rabex-5*^{ex42}, genomic sequence is present 135 bases prior to the start ATG (base

1295891 of the genomic sequence) and resumes at 1004 bases into the corresponding mRNA (1297241 of the genomic sequence).

Mosaic analysis: Expressing the FLP recombinase induces mitotic recombination at FRT sites. Expression of the FLP recombinase in cells carrying *FRT80B* with a wild-type chromosome or an *FRT80B* chromosome carrying a mutant allele of *Rabex-5* generates mosaic tissue containing cells homozygous for the wild-type *FRT80B* chromosome or cells homozygous for *Rabex-5*^{ex42} in the otherwise heterozygous fly. We created homozygous clones throughout the fly randomly using a *hsFLP* element and applying brief heat shock during development for analysis shown in Fig. S1E-G. Rather than generating mosaic tissue containing random clones as we did in the wing (S1E-G) using *hsFLP*, we also used the FLP/FRT system to generate mosaic eyes using an *eyFLP* element. To generate eyes composed primarily of we used an *FRT80B* chromosome carrying the *Minute* mutation *Mi55*. Cells containing *Minute* mutations grow poorly and are often eliminated in mosaic tissues. By generating a mosaic eye composed of *Rabex-5* mutant tissue and *Mi55* mutant tissue, of the genotype *y w eyFLP; FRT80B Rabex-5*^{ex42}*/FRT80B Mi55*, the poor growth of the *Mi55* mutant tissue would result in an eye with substantial or even primarily *Rabex-5* mutant tissue. *y w eyFLP; FRT80B Rabex-5*^{ex42}*/FRT80B Mi55* flies are shown in Fig. S1R-W'. To generate mosaic eyes containing either wild-type *FRT80B* homozygous control tissue or homozygous *Rabex-5*^{ex42}mutant clones for immunohistochemical analysis as shown in Fig. S1Y-Y'', we used the FLP/FRT system to generate flies of the genotype *y w eyFLP; FRT80B Rabex-5*^{ex42}*/FRT80BpW+ Ubi GFP*.

Tissue specific RNAi of *Rabex-5*: There are no reported strong or complete loss-of-function alleles of *Drosophila Rabex-5*. The Vienna *Drosophila* RNAi Center (VDRC) generated a gal4-inducible inverted repeat allele for *Rabex-5*, *P{GD14133}v46329 CG9139*^{GD14133}, referred to here as *Rabex-5*^{IR} [see reference 16 of the main text] which produces dsRNA to induce RNAi. In the gal4/UAS system, gal4 initiates transcription of Upstream Activating Sequences (UAS)-containing targets. Combining tissue-specific gal4 expression with a UAS-controlled transgene drives expression in desired patterns spatially and temporally [see reference 15 of the main text]. RNAi reduces gene expression; co-expressing *dcr2* achieves greater reduction but does not eliminate gene expression. To reduce *Rabex-5* constitutively at a low level, we crossed the *Actgal4* driver to the *Rabex-5*^{IR} allele (Fig. 1). To more strongly reduce *Rabex-5* levels constitutively, we crossed the *Actgal4* driver to the *Rabex-5*^{IR} allele in the presence of *UAS dcr2* (data not shown). To reduce *Rabex-5* in across the entire wing, we crossed the *c765gal4* driver to the *Rabex-5*^{IR} allele (Fig. 1). To strongly knock down *Rabex-5* in cells of the early eye, we crossed the *eygal4* driver to the *Rabex-5*^{IR} allele in the presence of *UAS dcr2* (Fig. 1). To reduce *Rabex-5* in differentiating cells in the eye, we crossed the GMRgal4 driver to the *Rabex-5*^{IR} allele (Fig. 2).

Engineering and over-expressing *Rabex-5* wild-type and mutant transgenes: The coding region of *Rabex-5* was cloned into pUAST with an N-terminal myc tag. Alanine substitutions at D313, P317, Y354, and T357 in mammalian *Rabex-5* inactivate Rab5 GEF activity (Delprato et al., 2004), so we made the alanine substitutions at conserved residues D316, P320, Y357, and T360 in *Rabex-5*^{DPYT}. Alanine substitution at the conserved Y25 Y26 in mammalian *Rabex-5* inactivates ubiquitin ligase activity (see reference 9 of the main text), so we engineered alanine

substitutions at the conserved F25 Y26 in *Rabex-5^{FY}* . Wild-type *Rabex-5, Rabex-5^{DPYT}*, and *Rabex-5^{FY}* were cloned into pUAST with N-terminal myc tags. Genetic Services, Inc. performed vector injection and isolated independent transgenic lines. We over-expressed the transgenes in the posterior compartment of the wing by crossing the *engal4* driver to each transgene (Fig. 3). We over-expressed the transgenes early in eye development by crossing each transgene to the *eygal4* driver, and later in differentiating cells in the eye by crossing the *GMRgal4* driver to each transgene.

Immunohistochemistry: Larvae were dissected and stained using standard protocols and imaged on a Leica TSC-SP confocal. Antibodies, anti-myc 9E10 (1:200, Santa Cruz Biotechnology), Alexa-Fluor 647 goat anti-mouse, Molecular Probes/Invitrogen.

Western Analysis: Larval extracts were prepared from individual larvae [21]. Westerns were visualized with the Li-Cor Odyssey. Antibodies, dpERK M8159 (1:2000), total ERK M5670 (1:2000) Sigma, anti-myc 9E10 (1:1000, Santa Cruz Biotechnology), anti-HA 12CA5 (1:1000, Roche), anti-FlagM2 (1:1000, Sigma), Alexa-Fluor goat anti-mouse 680 (1:20,000) and Alexa-Fluor goat anti-rabbit 680 (1:20,000), Molecular Probes/Invitrogen.

Tissue Culture. S2 cells cultured at 25°C were transfected with *pIE$^{1-4}$, pIE$^{1-4}$-Flag-6HisRas*, *Actin-Gal4*, *UAS-HA-Ubiquitin*, *UAS-myc-Rabex-5, pIE$^{1-4}$ DIAP1,* and/or *pAc5.1-FLAG-6His Rab5* using Cellfectin (Invitrogen). Ubiquitin conjugates were isolated from cell lysates as described [21]. To induce cell death, S2 cells were incubated with DMSO as a vehicle control, or the indicated concentrations of CHX and counted and stained with Trypan blue at 0 hours or 6

hours. Four samples were counted per well to ensure the precision of counting, and the entire experiment was performed in triplicate. Trypan blue was generously provided by Dr. J.E. Chipuk.

Statistics: Calculations were done in Excel. Student unpaired t-tests compared length, weight, wing area (Fig. 1D, Fig. S1C) and eye size (Fig. 4D). Unpaired t-tests assuming equal variance compared the levels of Trypan blue-positive cells between control-transfected and DIAP1-transfected wells (Fig. S4N) and between DIAP1-transfected cells undergoing different treatments, and paired t-tests compared the levels of Trypan blue-positive DIAP1-transfecteed cells at different time points. Paired t-tests compared ubiquitination levels (Fig. S4K). Chi-square or Fisher's exact tests compared PCV, LV, eye phenotypes, and lethality (Fig. 1K, 1P, Fig. S1D, S1G, S1X, Fig. 2C, 2H, Fig. S2I, S2J, S2K, S2S, Fig. 3E, Fig. 4D, and Fig. S4G).

Fly Genotypes from the images appearing in figures from the main paper:

w;FRT80B (Fig. 1A, left; Fig. 1B, left)

w; FRT80B Rabex-5^{ex42}/FRT80B Rabex-5^{ex42} (Fig. 1A, right; Fig. 1B, right)

w; Actgal4/+ (Fig. 1 C left; Fig. 1D blue; Fig. 1F)

w; UAS Rabex-5^{IR}/+; Actgal4/+ (Fig. 1C, right; Fig. 1E red; Fig. 1G,)

w; *c765gal4/+*(Fig. 1H)

w; *UAS Rabex-5^{IR}/+; c765gal4/+*(Fig. 1I)

w; *UAS Rabex-5^{IR}/+; c765gal4/FRT80B Rabex-5^{ex42}* (Fig. 1J)

UAS dcr2; eygal4/+ (Fig. 1L)

UAS dcr2; eygal4/UAS Rabex-5^{IR} (Fig. 1M-O)

w; *GMRgal4, UAS Egfr^{A887T}*/+ (Fig. 2A, left)

w; *GMRgal4, UAS Egfr^{A887T}/UAS Rabex-5^{IR}* (Fig. 2A, right)

w; *GMRgal4, UAS RasV12S35*/+ (Fig. 2B, left; Fig. 4A-C left)

w; *GMRgal4, UAS RasV12S35/UAS Rabex-5^{IR}* (Fig. 2B, right)

w; eygal4/+ (Fig. 2D)

w; eygal4/UAS Rabex-5^{IR} (Fig. 2E)

w; eygal4/UAS RasV12S35 (Fig. 2F)

w; eygal4, UAS Rabex-5^{IR}/UAS RasV12S35(Fig. 2G)

w; engal4/+ (Fig. 3A)

w; *engal4/UAS Rabex-5^{WT}* (Fig. 3B)

w; engal4/+ ;UAS Rabex-5^{DPYT}/+ (Fig. 3C)

w; engal4/+; UAS Rabex-5^{FY}/+ (Fig. 3D)

hsFLP; Aygal4/+;UAS Rabex-5^{DPYT}/+ (Fig. 3F-H)

w; *GMRgal4, UAS RasV12S35/UAS Rabex-5^{WT}* (Fig. 4A, right)

w; GMRgal4, UAS RasV12S35/+; UAS Rabex-5^{DPYT}/+ (Fig. 4B, right)

w; GMRgal4, UAS RasV12S35/+; UAS Rabex-5^{FY}/+ (Fig. 4C, right)

Fly Genotypes from the images appearing in the Supplemental Figures:

y w hsFLP; FRT80B pW+ UbiGFP/FRT80B (Fig. S1E)

y w hsFLP; FRT80B pW+ Ubi-GFP/FRT80B Rabex-5^{ex42} (Fig. S1F)

UAS dcr2; eygal4/+ (Fig. S1H)

UAS dcr2; eygal4/UAS Rabex-5^{IR} (Fig. S1I-Q)

y w eyFLP; FRT80B Mi55 UbiGFP/FRT80B (Fig. S1R, left)

y w eyFLP; FRT80B Rabex-5^{ex42}/FRT80B Mi55 (Fig. S1R, right; Fig. S1R'-W')

y w eyFLP; FRT80B pW+ Ubi-GFP/FRT80B Rabex-5^{ex42} (Fig. S1Y-Y'')

w; *GMRgal4, UAS RasV12S35/SM6-TM6B* (Fig. S2A, Fig. S2B, left)

w; *GMRgal4, UAS RasV12S35/GMRgal4, UAS RasV12S35* (Fig. S2B, right)

w; GMRgal4/+(Fig. S2D, right; Fig. S2E, right)

w; *GMRgal4, UAS Egfr^{A887T}/+* (Fig. S2D, left; Fig. S2G, left)

w; *GMRgal4, UAS RasV12S35*/+ (Fig. S2E, left; Fig. S2H, left)

w; GMRgal4/*UAS Rabex-5^{IR}* (Fig. S2F)

w; *GMRgal4, UAS Egfr^{A887T}/+; FRT80B Rabex-5^{ex42}* (Fig. S2G, right)

w; *GMRgal4, UAS RasV12S35/+; FRT80B Rabex-5^{ex42}* (Fig. S2H, right)

w; eygal4/+ (Fig. S2L)

w; eygal4/UAS Rabex-5^{IR} (Fig. S2M)

w; eygal4/UAS RasV12S35 (Fig. S2N)

w; eygal4, UAS Rabex-5^{IR}/UAS RasV12S35 (Fig. S2O-R)

w; *engal4/+* (Fig. S3A)

w; *engal4/UAS Rabex-5^{WT}* (Fig. S3B, Fig. S3E-G)

w; engal4/+ ;UAS Rabex-5^{DPYT}/+ (Fig. S3C)

w; engal4/+; UAS Rabex-5^{FY}/+ (Fig. S3D)

w; GMRgal4/UAS Rabex-5^{WT} (Fig. S4A, S4D)

w; GMRgal4/+; UAS Rabex-5^{DPYT}/+ (Fig. S4B, S4E)

w; GMRgal4/+; UAS Rabex-5^{FY}/+ (Fig. S4C, S4F)

Supplemental References:

Delprato, A., Merithew, E., and Lambright, D.G. (2004). Structure, exchange determinants, and family-wide rab specificity of the tandem helical bundle and Vps9 domains of Rabex-5. Cell 118, 607-617.

Wilson, R., Goyal, L., Ditzel, M., Zachariou, A., Baker, D.A., Agapite, J., Steller, H., and Meier, P. (2002). The DIAP1 RING finger mediates ubiquitination of Dronc and is indispensable for regulating apoptosis. Nat Cell Biol. 4, 445-50.

Hays, R., Wickline, L., and Cagan, R. (2002). Morgue mediates apoptosis in the Drosophila melanogaster retina by promoting degradation of DIAP1. Nat Cell Biol. 4, 425-431.

Ditzel, M., Broemer, M., Tenev, T., Bolduc, C., Lee, T.V., Rigbolt, K.T., Elliott, R., Zvelebil, M., Blagoev, B., Bergmann, A., and Meier, P. (2008). Inactivation of effector caspases through nondegradative polyubiquitylation. Mol Cell 32, 540-553.